Optical Flow Sensor for Continuous Invasive Measurement of Blood Flow Velocity

Albert Ruiz-Vargas [1,2], *Scott A. Morris* [2,3], *Richard H. Hartley* [4] *and John W. Arkwright* [1*]

*Corresponding Author: E-mail: john.arkwright@flinders.edu.au

[1]The Medical Device Research Institute, College of Science and Engineering, Flinders University, Tonsley 5042, Australia
[2]College of Medicine and Public Health, Flinders University, Bedford Park 5042, Australia
[3]Neonatal Unit, Flinders Medical Centre, Bedford Park 5042, Australia
[4]Independent Researcher, Adelaide, Australia

ABSTRACT (UP TO 200 WORDS)

Continuous monitoring of intrapulse measurement of blood flow in humans is currently not achievable with clinically available instruments. In this paper, we demonstrate a method of measuring the instantaneous variations in flow during pulsatile blood flow with an optical flow sensor comprising a fiber Bragg grating sensor and illumination from a 565 nm Light-Emitting-Diode. The LED illumination heats the blood and fluctuations in temperature, due to variations in flow, are detected by the fiber sensor. A set of experiments at different flow rates (20 to 900 mL/min) are performed in a simulated cardiac circulation setup with pulsatile flow. Data are compared with an in-line time of flight ultrasound flow sensor. Our results show that the optical and ultrasonic signals correlate with Pearson coefficients ranging from -0.83 to -0.98, dependent on the pulsatile frequency. Average flow determined by ultrasound and the optical fiber sensor showed a parabolic

This article has been accepted for publication and undergone full peer review but has not been through the copyediting, typesetting, pagination and proofreading process, which may lead to differences between this version and the Version of Record. Please cite this article as doi: 10.1002/jbio.201900139

relationship with R^2 = 0.99. An abrupt step change in flow induced by occlusion and release of the circuit tubing demonstrated that the optical fiber and ultrasound sensor had similar response. The method described is capable of intrapulse blood flow measurement under pulsatile flow conditions, with potential applications in medicine where continuous blood flow sensing is desired.

Abstract figure: (it should be a short descriptive and popular text on the general aim and value of the paper, suggest image 5x5 cm, up to 70 words)

Limitations of current methods for monitoring blood flow in a continuous manner urge the necessity of developing new methods for clinical environments. A new method consisting for monitoring temperature fluctuations by subtle optical heating of the blood is proposed here. The method will allow the measurement of intrapulse blood flow in humans for different clinical environments and biomedical applications.

KEYWORDS:

blood flow, light absorption, fiber Bragg grating, continuous measurement

INTRODUCTION

In a medical setting, the measurement of blood flow is relevant for research and clinical applications, particularly where changes to flow are dynamic as is often the case in surgical or intensive care environments [1], [2]. The most widely used technique to assess blood flow is ultrasound which has significant limitations

including being restricted to intermittent measures of blood flow, and precision and accuracy errors, due in part to inter-operator variability [3].

Other options, such as thermodilution catheters and magnetic resonance imaging (MRI), exist to objectively measure blood flow from heart and smaller arteries and veins in human body [1]. However, the thermodilution technique generally requires the injection of considerable volumes of fluid into the circulatory system [4], and MRI is complex and expensive. Measurement of 'continuous' blood flow using hot wire convective heating of blood is currently available technology although such devices only provide averaged flow. Continuous intrapulse (instantaneous) measurement is not possible. Such devices also have significant disadvantages in catheter size, positioning in the pulmonary artery and the need for electrical heating of components.

Measuring instantaneous blood flow, as opposed to averaged blood flow, is appealing because of the potential for rapid fluctuations in organ blood flow which may be undetected by conventional monitoring devices yet have consequences for organ injury [5], [6].

Here, we present a new method to monitor blood flow, which consists of applying pulses of light from a low power light emitting diode (LED) at a specific wavelength of 565 nm. This causes instantaneous heating of hemoglobin via optical absorption, that can be detected by a fiber Bragg grating (FBG) element.

The advantages of heating blood by light absorption are rapid heating and high sensitivity to pulsatile flow changes, and the lack of electrical components. The use of an optical fiber sensing element as a temperature sensor has advantages including small size, high flexibility, immunity to electromagnetic interference, high sensitivity and stability [7].

This paper describes the probe design, and in-vitro experiments that aim to determine the feasibility of optical heating and temperature sensing of human blood to detect blood flow.

MATERIALS AND METHODS

Probe

Figure 1 shows the optical flow sensor developed for performing the measurements. It consists of a multimode fiber with an outer diameter of 730 μm (FT400UMT, Thorlabs, Newton, New Jersey, USA) to guide LED light, and an adjacent single mode optical fiber containing an FBG element (DTG, FBGS, Geel, Belgium) to measure temperature change. The multimode and single mode fibers were connectorized with SMA and E-2000 connectors respectively.

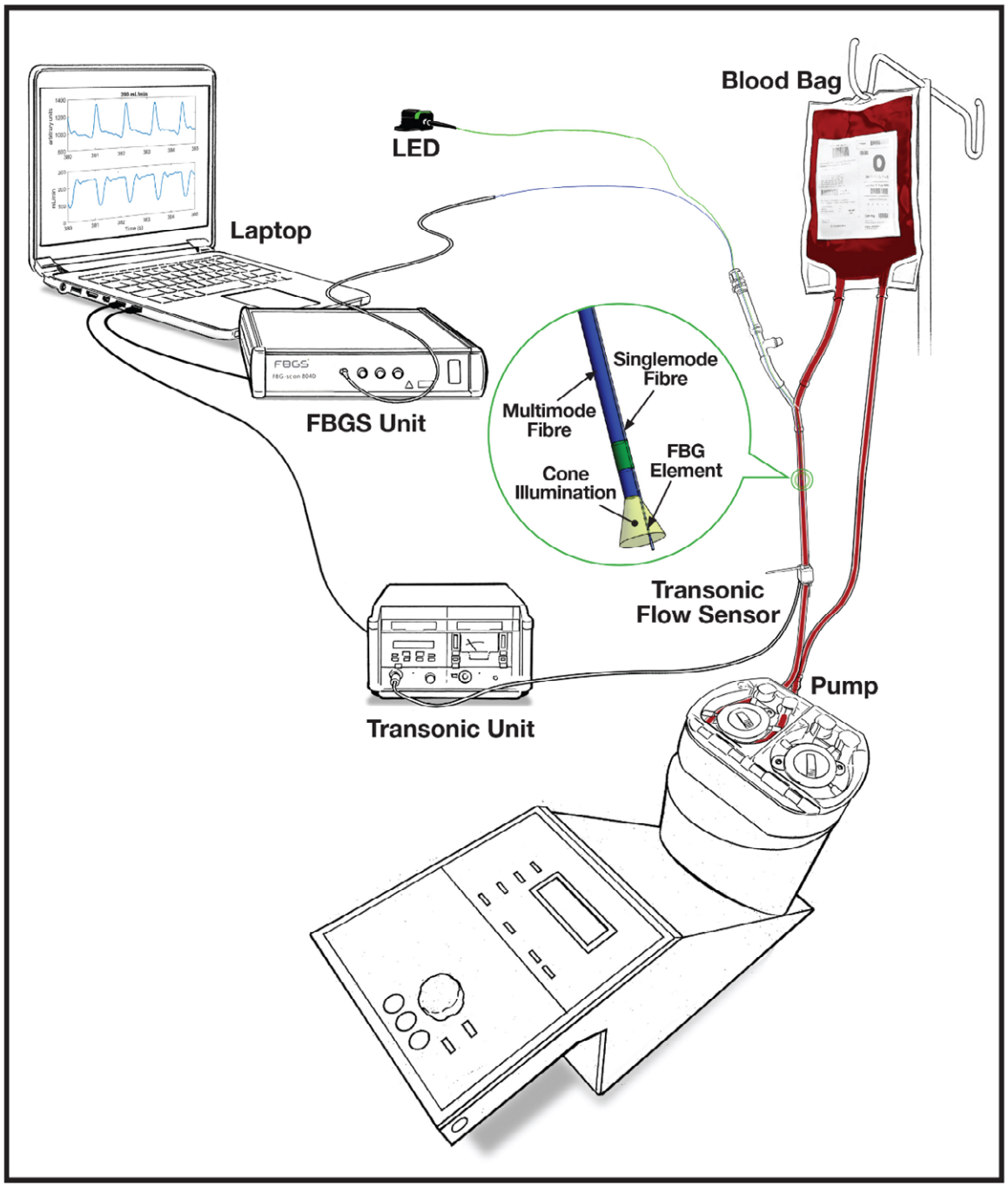

Figure 1. Representation of the optical flow sensor probe and schematic representation of the set up

Equipment

Figure 1 also shows a schematic representation of the equipment used in the experimental set-up. A fiber-coupled LED with a wavelength of 565 nm and a maximum output power of 9.9 mW was launched into the multimode fiber (M565F3, Thorlabs, Newton, New Jersey, USA) and the center wavelength of the FBG was monitored using a spectral interrogator (FBGS-scan 804D, FBGS International, Geel, Belgium) with wavelength range of 1510 – 1590 nm. The intensity of the 565 nm radiation emitted from the multimode fiber was 4.1 mW/cm^2; measured with an optical power meter (Newport Model 1815–C, Newport Corporation, Irvine, California, USA) and calibrated photodiode sensor (Newport Model 818 – SL, Newport Corporation, Irvine, California, USA). The simulated circulation system consisted of a 2 m loop of Extracorporeal Circulation noDOP blood line tubing (1/4 x 1/16 inch, Raumedic®, Helmbrechts, Germany) with both extremes connected to a 1 L bag containing expired blood from the Flinders Medical Centre blood bank (Figure 1(b)). The system was closed to allow recycling of the blood. The blood was pumped through the system by means of a Stockert roller pump (Stockert SIII, Stockert, Munich, Germany). The circulation system is divided conceptually into two segments: one being ‘arterial’ (carrying fluid away from the peristaltic pump and into the bag) and one ‘venous’ (returning fluid from the bag to the pump).

Note that the roller pump is designed to deliver a constant average flow which can be varied from 0 to 1500 mL/min. Small fluctuations in flow (pulses) are however produced by the rotating peristaltic pump. Higher flow rates are produced by a higher

frequency of rotation of the pump, and hence as flow rate is increased, the pulse frequency also increases.

The optical sensor was inserted into the venous tubing through a gland seal and Y-junction. In addition, an inline flow meter (ME6PXN, Transonic®, Ithaca, NY, USA) – Transonic Flow Sensor (TFS) – was inserted in series into the venous tubing and distal to the tip of the optical sensor to acquire the instantaneous flow for comparison with the optical probe. The flow signal from ultrasonic sensor was acquired through a PowerLab acquisition module and the LabChart data analysis software (ADInstruments, Dunedin, New Zealand).

Custom software was developed in National Instruments LabVIEW (version 2015 sp1, National Instruments, Austin, Texas, USA) to control the LED driver (LEDD1B, Thorlabs, Newton, New Jersey, USA) and to acquire and process the change in wavelength of the FBG. An edge filter algorithm (described below) was used to detect changes in intensity as the FBG peak moved. This gave a higher sensitivity to spectral shifts than the peak tracking algorithm incorporated in the firmware of the interrogator.

The data acquisition rates for optical and ultrasonic sensors were 100 Hz and 1 kHz respectively.

Edge detection algorithm

The temperature sensitivity of the FBG element using peak wavelength tracking is limited to 15 pm/ºC. The wavelength sensitivity of the optical interrogator is limited to

1 pm by its analog-to-digital converter, hence this sensitivity is insufficient to detect changes of temperature less than 0.066 ºC. To increase the sensitivity of the measurement, an edge detection algorithm was used. The algorithm consists of finding the maximum peak power(s) (P_2) along the 512 pixels on the CCD, and then recording the change in power (ΔP) of the nearest neighbor or next-nearest neighbor pixel as an indicator of temperature change. The sensitivity was further enhanced by computing the power difference from the neighboring pixels (pixel 1 and 3) on either side of the maximum peak (see Figure 2(a)) as shown in Equation 1 and 2:

$$P_d = \Delta P_1 - \Delta P_3 \quad (1)$$

$$P_d = (P_1 - P_{1'}) - (P_3 - P_{3'}) \quad (2)$$

Where ΔP_n are the power increment for the next-nearest neighbor pixels, $P_{n'}$ are the time varying power of pixels, P_n are the initial power of pixels and P_d is a measure of the spectral shift. Using this technique, thermal shifts less than 0.001ºC can be detected.

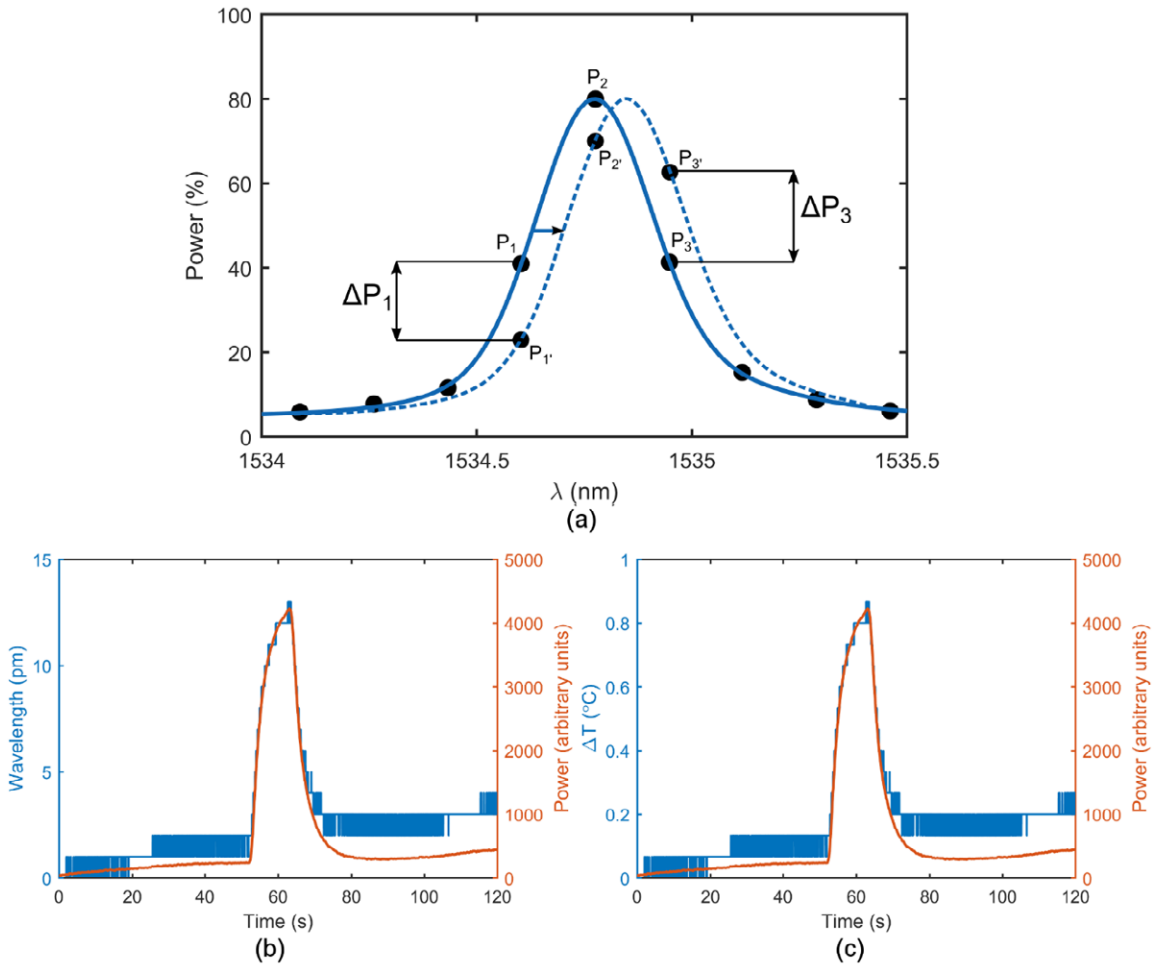

Figure 2. (a) Representation of edge detection algorithm (the continuous line represents the spectrum at the initial point and dashed line represents the spectrum line after temperature changed): P_n are the initial power of pixels and $P_{n'}$ are the current power of pixels, ΔP_n are the power increments of the pixels on each side of the peak (b) Resolution by using edge detection technique as opposed to use wavelength tracking. Left graph shows the change in peak wavelength and power due to temperature effect, and right graph shows the peak wavelength converted into temperature and the power.

Experimental protocol

For this experiment, expired human blood transfusion packs were obtained from Flinders Medical Centre Transfusion Service. Ethical approval was obtained from the

Southern Adelaide Clinical Human Research Ethics Committee (ethics approval no. 49.48).

The cardiac circulation circuit was primed with care to exclude air bubbles. Furthermore, to minimize turbulent flow the tubing was kept straight, and the Y-junction was kept at a distance at least 5 times the tubing diameter from the fiber optic sensor and transonic flow sensor.

Saline water was used as a control fluid to confirm that any optical heating effect was due to the absorption of blood. Once the optical flow sensor was in the circulation system and with no flow, the LED was turned on for 50 seconds.

Prior to starting the experiment with blood, the TFS was calibrated by setting the roller pump at 0 and 500 mL/min and recording the TFS output voltages at those specific flow rates. Once the TFS was calibrated with the roller pump, the protocol was as following:

1. Turning the LED on for 100 seconds at 0 mL/min to establish a baseline measurement.
2. Flow rates at 20, 50, 70, 100, 120, 150, 170 and 200 mL/min were set on the roller pump and the LED was turned on for 50 seconds for each flow rate to capture multiple flow pulsations from the rotating spindle of the peristaltic pump.
3. Then flow was increased in increments of 100 mL/min from 300 to 900 mL/min, with the LED on for 20 seconds at each increment.

Note that time stamps were added to the data when LED was on and off in both software programs (LabVIEW app and LabChart) to synchronize the data for ease of analysis.

Hemoglobin concentration and oxygen saturation of the blood in the circuit were measured with an ABL800 Flex blood gas analyzer (Radiometer Medical, Denmark), and blood temperature was measured using an electronic thermometer (Fluke model 1523, Fluke Corporation, Everett, WA, USA).

Post Processing and Validation

Data obtained from both sensors were analyzed with a script developed in Matlab (MathWorks, Natick, Massachusetts, USA). Data from the optical sensor was interpolated to match the highest frequency of the ultrasonic sensor (1 kHz) and then compared at each specific flow rate from 20 to 900 mL/min. Fundamental frequency of the pulsatile flow was determined at each flow rate. Both signals were synchronized, and instantaneous outputs from each instrument over 3 pulse cycles were correlated using Pearson's correlation coefficient (PCC). Three cycles were used at each flow rate to compute the average signal using area under the curves. Average signals at each flow rate from the optical and ultrasonic sensors were fitted in a model using 4-parameter-logistic regression. The equation derived was used to convert optical power in arbitrary units to flow in mL/min. The response of the both sensors to sudden changes in flow was tested by causing transient occlusion of the arterial or venous tubing.

RESULTS AND DISCUSSION

The hemoglobin concentration of the blood was 160 g/L, fractional oxygen saturation 59.3%, and temperature 23.5°C. Figure 3 shows the increase in power due to temperature increase for the optical fiber sensor under conditions of stasis in the tube when the LED light was turned on. As expected, blood absorbed light at the specific wavelength of 565 nm and increased in temperature, whereas saline showed minimal optical absorption and heating.

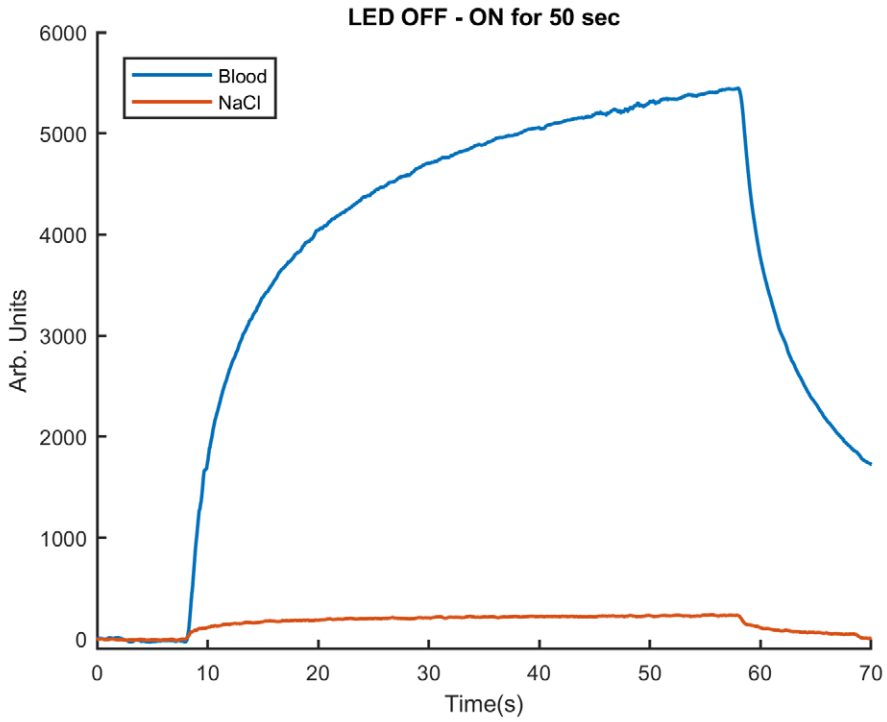

Figure 3. Results of applying 565 nm for 50 seconds with no flow in saline solution and blood. This represents a temperature change approximately of 1.1º C.

Figure 4 shows the complete recording before, during and after the LED was on for 50 seconds at a flow rate of 50 mL/min. Temperature was shown to increase when the LED was switched on and fluctuated due to changes in pulsatile flow velocity. Increases in temperature correlated with slowing of flow, and hence the signal from the TFS was mirror image to the signal from the optical sensor.

Pulsatile variations were seen for all flow rates, but the optical signal was less well defined at higher flow (and pulse) rates when limitations in thermal response time of the optical sensor became evident. This change in signal quality at higher pulse frequencies was also evident for the TFS as shown in Figure 5 (see also Supplementary information for recordings at different flow rates and pulse frequencies). Table 1 shows the fundamental frequency, average area and PCC results obtained from the data at different flow rates. Generally, the PCC between optical and ultrasonic signals are above -0.9 except for flow rates above 700 mL/min that drops below -0.9.

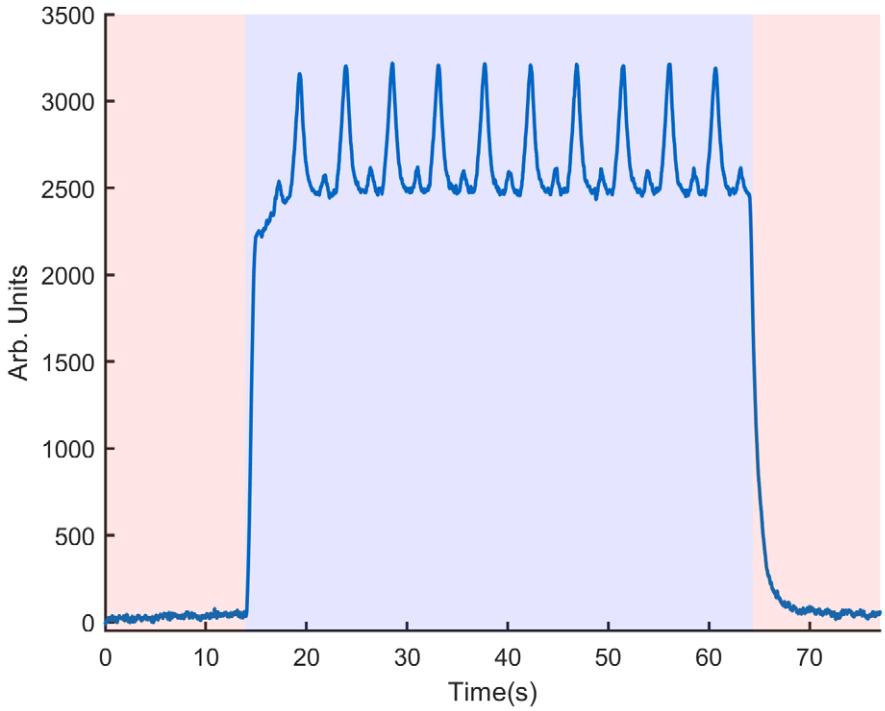

Figure 4. Recorded signal from the optical signal before, during and after applying LED on at a flow rate of 50 mL/min.

Flow (mL/min)	Frequency (Hz)	Area		PCC
		OFS (arb. units)	TFS (mL/min)	
20	0.065	3548.933	17.66	-0.93
50	0.227	2417.620	51.73	-0.96
70	0.316	2028.470	74.22	-0.96
100	0.416	1757.851	100.07	-0.97
120	0.500	1527.303	125.21	-0.97
150	0.666	1335.386	154.6	-0.97
170	0.777	1256.574	172.95	-0.97
200	0.856	1143.540	198.58	-0.97
300	1.284	916.640	301.08	-0.98
400	1.796	731.500	402.54	-0.95
500	2.138	579.641	498.00	-0.93
600	2.662	441.990	600.05	-0.97
700	2.965	355.505	702.87	-0.96
800	3.418	295.936	799.02	-0.88

900	4.050	248.990	897.46	-0.83

Table 1. Results from the optical fiber sensor (OFS) and Transonic flow sensor (TFS) at each flow rate with its corresponding, fundamental frquency, average area and Pearson correlation coefficient between optical and ultrasonic signals.

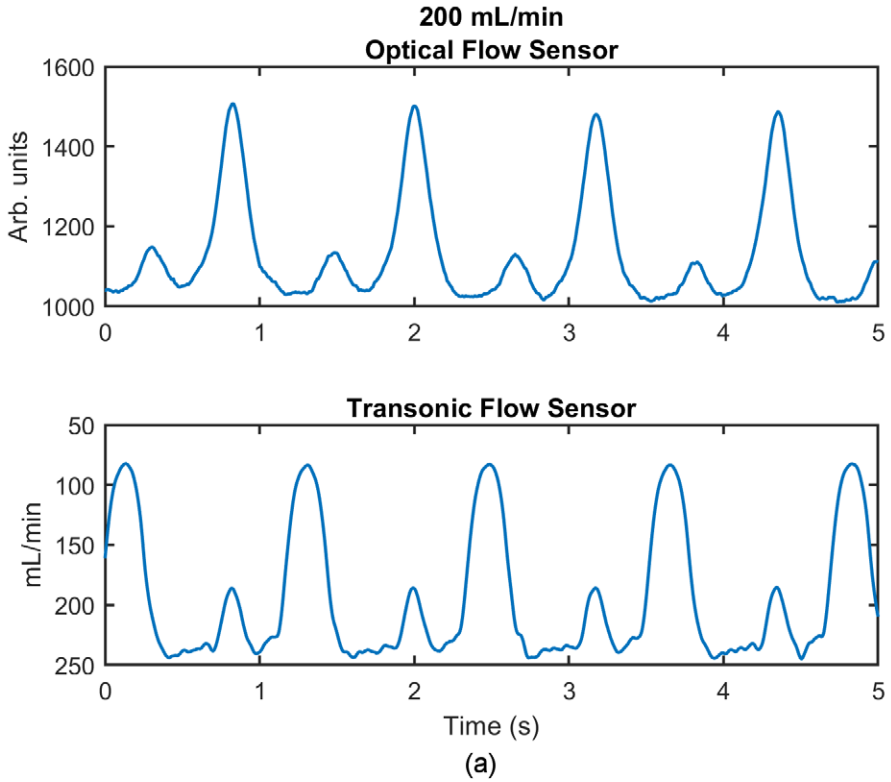

(a)

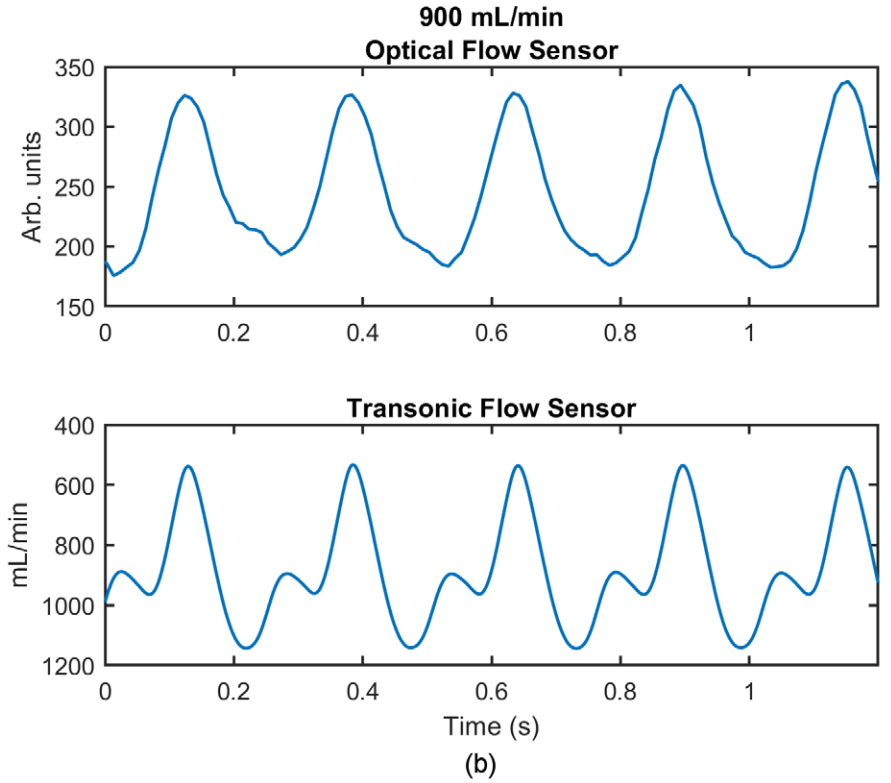

(b)

Figure 5. Results of instantaneous temperature change from the optical sensor in arbitrary units of optical power output (top graph) and instantaneous flow from the ultrasonic sensor (bottom graph) at (a) 200 mL/min and (b) 900 mL/min. The delay between optical and ultrasonic signals is due to the different positions of the sensors in the circulation circuit. Note that the y-axis of ultrasonic graphs has been inverted, because increments in power due to temperature occur when fluid velocity decreases.

Figure 6 shows the output power and flow rate from averaging area under the curves from three consecutive cycles of the optical and ultrasonic signals, respectively, fitted using 4 parameter logistic regression.

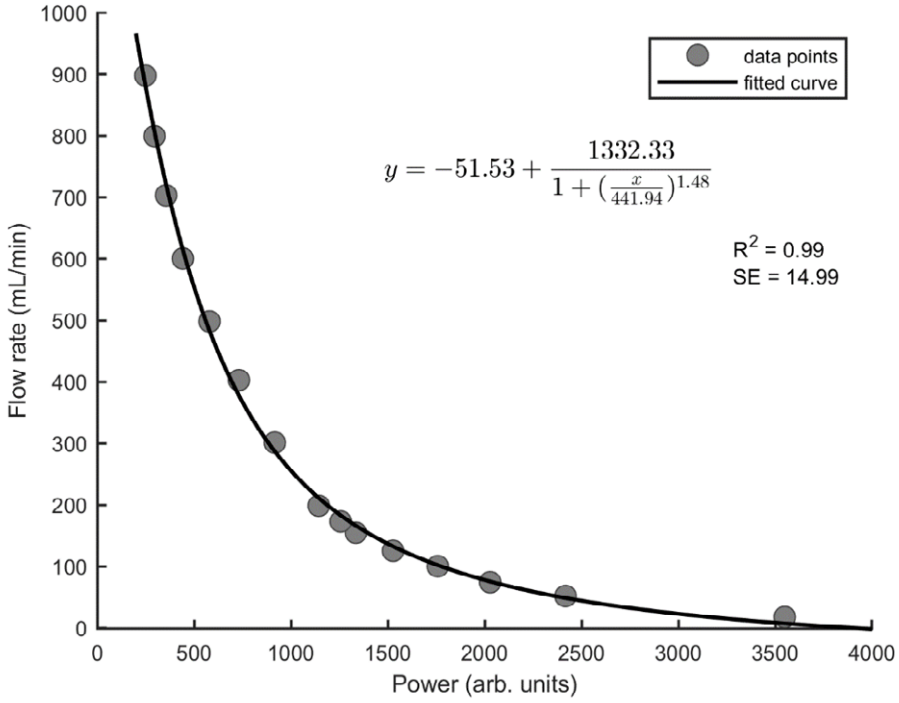

Figure 6. Characterization of optical sensor with respect of ultrasonic sensor for flow rates from 20 to 900 mL/min. Y axis represents the flow rates obtained from the TFS; and x axis represents the change in power (in arbitrary units) due to the change in temperature. The equation shows the curve fit to the measured data and is used to convert optical data into flow rate, where '*x*' corresponds to the values

from the optical flow sensor in arbitrary units and '*y*' the values from the optical flow sensor converted into flow rate units in mL/min.

The equation derived from modelling was used to determine flow rate in mL/min from the optical data in arbitrary units. Figure 7 shows the effect of sudden occlusion of circuit tubing followed by release, on flow determined by the ultrasonic and optical sensors in mL/min (optical data in arbitrary units were converted into mL/min using the equation obtained in Figure 6). Sudden changes in flow were detected in a similar fashion by both the optical and the ultrasonic sensor.

The average flow rate for the ultrasonic signal (gold standard method in this study), illustrated in Figure 7, is 131.62 mL/min and the average flow rate for the optical sensor is 147.22 mL/min; hence the error in this instance for the optical sensor measurement was approximately 11% with respect to the gold-standard measurement.

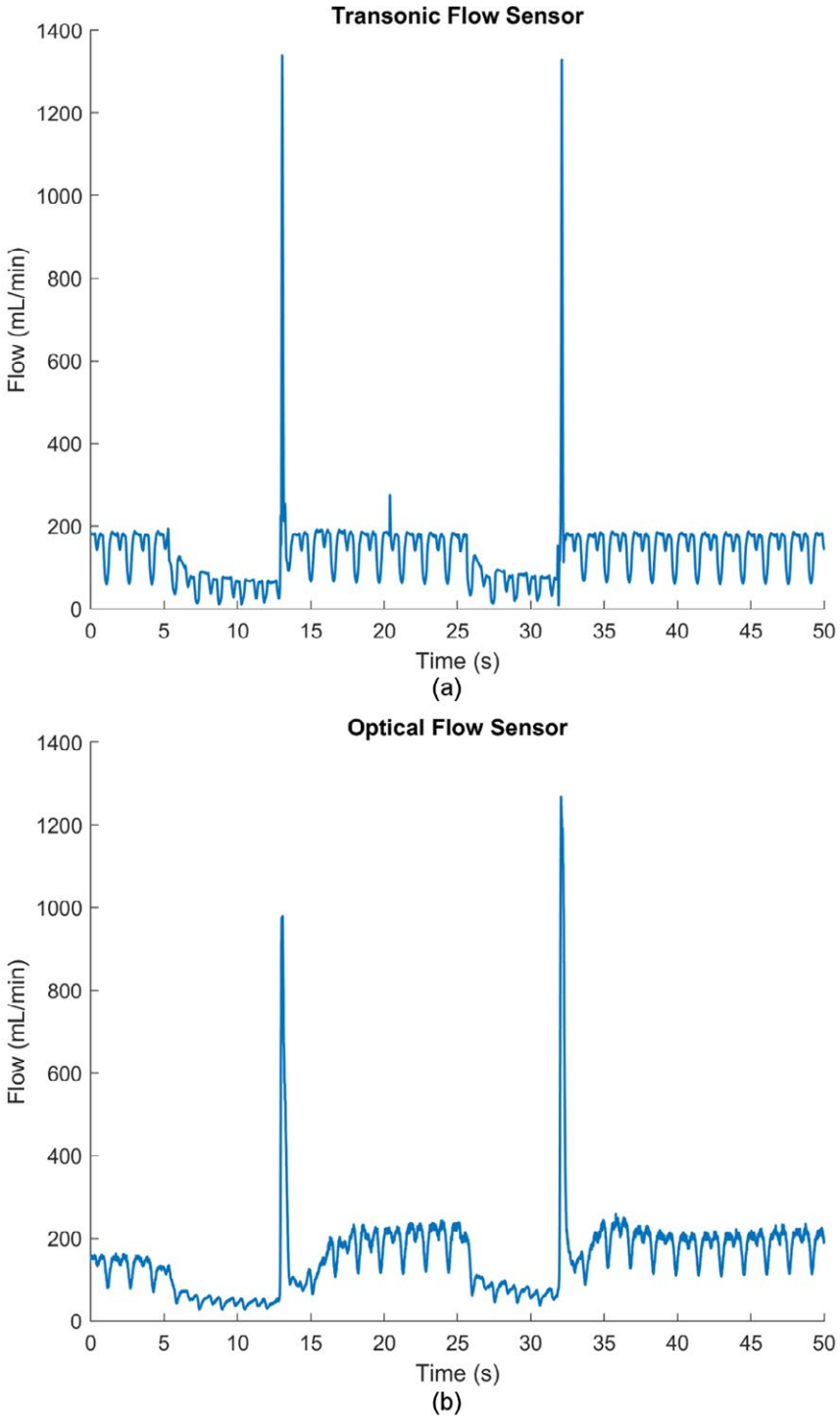

Figure 7. Comparison between the ultrasonic flow sensor and optical flow sensor (after optical signal data was converted into flow rates with the fitted curve) during two occlusion episodes. The first occlusion occurred at 5 seconds decreasing flow rate followed by release at 13 seconds. A significant

increase in flow (spike) is noted. The second occlusion occurred at 25 seconds followed by release at 32 seconds and a flow spike.

These results demonstrate the feasibility of continuous and instantaneous sensing of blood flow using optical heating at a low power input with an LED light source, and temperature sensing using FBG and spectral edge detection. The small sensor dimensions and minimal heating of blood suggest that the concepts is applicable to blood flow measurement in vivo.

Our study is the first demonstration that optical heating of blood and temperature sensing using FBG is capable of continuous measurement of intrapulse (instantaneous) flow velocity. This has potential importance in a medical environment, where typical monitoring of blood flow gives intermittent and averaged values. Spike events such as that induced by occlusion of the plastic tubing in our experiments would not be seen by an averaged value measurement. Instantaneous measurement opens the possibility of continuous beat-to-beat measurement of flow variations.

The data also show that under the experimental conditions applied, the area under the curve of temperature change has a defined mathematical relationship to flow measured accurately by ultrasound. These preliminary data are important in showing proof of concept. However, this relationship is likely to be specific to our conditions and to be influenced by multiple variables. Limitations include the specific temperature, haemoglobin saturation and haemoglobin concentrations used which are different to normal physiological values. Variations in these values will influence

light absorption by haemoglobin and localised heating of blood close to the FBG sensor. Plastic tubing exposed to ambient temperature can also be expected to result in different rates of heat loss to the environment when compared to a vessel within the human body. The calibration curve we have derived is therefore not directly applicable to an in-vivo environment. For in-vivo measurements, the optical sensor could be calibrated against Doppler ultrasound to provide a quantitative value of flow at the start of the measurement. However further studies are required to determine the performance and calibration requirements of the proposed sensor under physiological conditions.

The study was limited by the roller pump because flow rate and pulse frequency could not be independently varied. Hence at 20 mL/min the pulse frequency is 4 bpm, and at 900 mL/min pulse frequency is 240 bpm. At higher pulse frequencies, limitations in the sensor response time to temperature change reduced signal quality such that instantaneous flow measurement became less reliable. However at flow rates of 200-500 mL/min and pulse frequencies in the range of 60-120 bpm, which approximate values in the human neonate, the optical signal correlated well with the ultrasonic signal [8]. Cardiac output in an adult approximates 5.5 L/min, and the high pulse frequency generated by the roller pump to achieve such flows precluded the ability to explore physiological flow rates in adults [8], [9]. Further work on conditions, where heart rate is likely to be raised is required.

We also used a constant LED power (4.1 mW), and wavelength (565nm). The performance of wavelengths with differing spectral absorption and powers requires future exploration.

CONCLUSION

We have described for the first time a means to continuously measure intrapulse blood flow using a fiber optic sensor which has the potential to advance monitoring in a medical setting. More research is required to determine how the sensor will behave under more physiological conditions and to examine different encapsulations to comply with human safety.

ACKNOWLEDGEMENTS

This work was supported by a Flinders Foundation small competitive research grant 2016, a Flinders University near miss grant, and a grant from the Southern Adelaide local Health Network Clinician's Special Purpose Fund.

The authors would like to thank Richard Newland and Rob Baker from the Cardiac and Thoracic Surgical Unit at Flinders Medical Centre for their help setting the experimental set up and revising the method section.

REFERENCES

[1] L. Busse, D. L. Davison, C. Junker, and L. S. Chawla, 'Hemodynamic Monitoring in the Critical Care Environment', *Adv. Chronic Kidney Dis.*, vol. 20, no. 1, pp. 21–29, 2013.

[2] M. Cannesson, G. Pestel, C. Ricks, A. Hoeft, and A. Perel, 'Hemodynamic monitoring and management in patients undergoing high risk surgery: A survey among North American and European anesthesiologists', *Crit. Care*, vol. 15, no. 4, p. R197, Aug. 2011.

[3] K. A. de Waal, 'The Methodology of Doppler-Derived Central Blood Flow Measurements in Newborn Infants', *Int. J. Pediatr.*, vol. 2012, no. 3, pp. 1–13, 2012.

[4] X. Monnet and J. L. Teboul, 'Transpulmonary thermodilution: Advantages and limits', *Crit. Care*, vol. 21, no. 1, pp. 1–12, 2017.

[5] M. Kluckow and N. Evans, 'Superior vena cava flow in newborn infants: a novel marker of systemic blood flow', *Arch. Dis. Child. Fetal Neonatal Ed.*, vol. 82, no. September 1999, pp. 182–187, 2000.

[6] R. W. Hunt, N. Evans, I. Rieger, and M. Kluckow, 'Low superior vena cava flow and neurodevelopment at 3 years in very preterm infants', *J. Pediatr.*, vol. 145, no. 5, pp. 588–592, 2004.

[7] F. Baldini, A. Giannetti, A. A. Mencaglia, and C. Trono, 'Fiber optic sensors for biomedical applications', *Curr. Anal. Chem.*, vol. 4, no. 4, pp. 378–390, Oct. 2008.

[8] C. Wu *et al.*, 'Age-related changes of normal cerebral and cardiac blood flow in children and adults aged 7 months to 61 years', *J. Am. Heart Assoc.*, vol. 5, no. 1, pp. 1–13, 2016.

[9] W. H. Fares *et al.*, 'Thermodilution and Fick cardiac outputs differ: impact on pulmonary hypertension evaluation.', *Can. Respir. J.*, vol. 19, no. 4, pp. 261–6, 2012.